

Performance Analysis of Elliptical Journal Bearing Lubricated with Experimentally Characterized Nano-lubricant Considering Thermal Effect Using CFD Technique

Basim A. Abass

Professor
University of Babylon
College of Engineering
Mechanical Eng. Dept.
Iraq

Saba Y. Ahmed

Professor
University of Babylon
College of Engineering
Mechanical Eng. Dept.
Iraq

Mohamed A. Yaser

University of Babylon
College of Engineering
Mechanical Eng. Dept.
Iraq

This study uses computational fluid dynamics (CFD) to quantitatively examine the performance of an elliptical journal bearing (EJB) lubricated with TiO_2 and ZnO nano-lubricant considering thermal effect. In an experiment, nanoparticles with particle concentrations varying from 0 to 2 weight percent are mixed with SAE15W40 engine oil to create these lubricants. The impact of weight fractions, rotational speed, eccentricity, and ellipticity ratios on the thermal performance of the EJB has been examined. The Kreger-Dougherty model is employed to understand the effects of oil film temperature as well as nanoparticle concentration on lubricant viscosity. The pressure and temperature determined by (Dang 2020) and (Wang 2021) were evaluated against the CFD model with good agreement. The findings show that for 2 wt% nanoparticles, ϵ of 0.6 and N of 5000 rpm, the load-carrying capacity increased by 5.5% and 4% and the side leakage flow decreased by 24.4% and 18%.

Keywords: EJB, nano-lubricants, Zinc Oxide (ZnO), Titanium dioxide (TiO_2), Thermal effect, CFD.

1. INTRODUCTION

Different configurations of plain bearings are used in rotating machinery and power generation appliances. The elliptical bearing is characterized by cooler oil film with more stability at higher velocities than the circular one. It was commonly used in turbo sets of small and medium ratings, steam turbines, and generators.

Many works have been conducted concerning the thermal effect on the performance of such bearings using different numerical and experimental techniques. Hussain et al. [1], examined the heat effect on circular and noncircular bearings. It was found that the EJB and the two-lobe bearing have the lowest and the highest load-carrying capacities, respectively. It was also discovered that, in contrast to these bearings, the load carried by the circular bearing is more sensitive to fluctuations in eccentricity ratio. In contrast, the ellipticity ratio has the dominant effect on the load carried by noncircular bearings. The isothermal and thermal performance of an elliptical bearing was numerically evaluated by Mishra [2]. It was found that pressure and temperature decreased as the ellipticity ratio increased due to the thick oil film. Additionally, it was also established that the isothermal pressure was higher than the thermal pressure. The side leakage and the friction coefficient decreased as the ellipticity ratio increased. The thermal behavior of an EJB lubricated with different grades of oil was discussed by Chauhan

and Sharma [3] using the finite difference method. An increasing pressure and temperature with the bearing's speed and eccentricity ratio and a decrease of those parameters with the elliptical ratio have been noticed. Experimental evaluation of the thermo-hydrodynamic performance of various kinds of oil-lubricated elliptical journal bearings was conducted by Sehgal [4]. It was noted that the rotational speed, loads, and oil types affected the thermal behavior of these bearings. In another work, Sehgal et al. [5] conducted an experimental measurement of the oil film temperature of EJB lubricated by Mak 2T, Hydro oil 68, and Mak Multigrade oils while operating at different loads and speeds. The obtained data demonstrated that the temperature and lubricant flow increased with the applied load and speed. Additionally, it was observed that a lower temperature was obtained when using Mak 2T Oil. Using a three-dimensional CFD approach, Susilowati et al. [6] investigated the laminar and turbulent behavior of a circular journal bearing numerically. The numerical simulation shows that the velocity impacts the bearing pressure. Additionally, it was shown that both laminar and turbulent regimes exhibit a similar tendency in the distribution of static hydrodynamic pressure. Singla and Chauhan [7] evaluated the oil film pressure and temperature at the mid-plane of a finite EJB working under different loads and lubricated with several grades of HYDROL oil. It was shown that the pressure and temperature increased with the applied load. It has been noted that oil grade HYDROL 68 gives the maximum increase in pressure and temperature under all working conditions compared to other lubricating oil grades. The impact of the eccentricity ratio on the friction force, load, and hydrodynamic pressure of a circular plain bearing was studied by Susilowati et al. [8] using the

Received: June 2023, Accepted: September 2023

Correspondence to: Professor Saba Y. Ahmed,
College of Engineering, Mechanical Engineering
Department, University of Babylon, Babylon, Iraq.
E-mail: eng.saba.yassub@uobabylon.edu.iq

doi: 10.5937/fme2304550A

© Faculty of Mechanical Engineering, Belgrade. All rights reserved

FME Transactions (2023) 51, 550-563 550

CFD technique. It was found that at higher eccentricity ratios, the bearing pressure and the load have been increased. The response of the EJB pressure, load, and temperature for different geometrical parameters was studied by Ebrahimi et al. [9]. It was noticed that while these parameters rose with the eccentricity ratios, an increase in non-circularity produced a drop in the highest oil film pressure temperature, in addition to the friction force. The variations in the load's direction and the bearing's primary axis's angle also result in decreased load and pressure and increased friction coefficient. Using an appropriate computer program created in MATLAB, Kumar et al. [10] examined the impact of an elliptical bearing's geometrical characteristics on the load and the film thickness. The findings show a pressure rise in the eccentricity ratio. Using an elliptical journal bearing with varying loads, speeds, and constant feeding pressure, Bhaskera et al. [11] investigated the experimental effect of Hydro oil 68 grade on the bearing performance. The results revealed an improvement in temperature and pressure distributions due to operating at constant speed and variable loads. Wang et al. [12] studied the impact of the non-circularity on the performance of an EJB while considering the cavitation effect using a mixed two-phase flow model. According to the data, elliptical bearings experience a lower maximum temperature rise than cylindrical ones. Additionally, the upper and lower lobes' highest pressure rises when the ellipticity grows. The EJB was discovered to transfer heat more effectively than the cylindrical bearing. The bearing's lubrication becomes crucial for improving performance once it has been built and put into use. Thus, altering the oils used to lubricate these bearings becomes a more efficient way to accomplish this. In order to account for the heat effect, Kedziński [13] examined a circular journal bearing lubricated with Nano-sized Al_2O_3 , Cu, Si, Al, and CuO lubricants. According to the investigation, the increased heat capacity of the Nano-lubricant led to an improvement in the journal-bearing performance. The thermal performance of an elliptical bearing lubricated with Nano-lubricant based on TiO_2 and CuO with 0.5, 1, and 2wt% dispersed in three different grades of mineral oils and working at variable speeds and eccentricity ratios was evaluated by Dang et al. [14]. The Nano-lubricant effect on the oil's thermo-physical characteristics was considered. The governing equations were simultaneously solved for pressure, temperature, and power loss evaluation. Temperature and nanoparticle concentration impacts on the lubricant viscosity were taken into account using the Krieger-Doherty viscosity model. It was observed that the maximum value of the pressure and load increased with higher nanoparticle concentrations and viscosity-grade lubricants. The circular journal bearing thermo-hydrodynamics performance when lubricated with TiO_2 and Al_2O_3 Nano-lubricants considering cavitation effect using CFD technique was studied by Saba et al. [15]. The obtained results demonstrate that the maximum pressure increased by 21%. Shooroki et al. [16] stated that applying Nano-lubricant to journal bearings is expected to enhance steady-state performance parameters such as load-carrying capacity, attitude angle,

surface cooling, and effective viscosity. The heating effect of two-lobe bearing lubricated with SiO_2 and multiwall carbon nanotubes distributed in SAE40 oil has been examined using the traditional Reynolds equation model. The performance of a bearing with various levels of non-circularity was examined in relation to the effect of the nanoparticle volume percent. An improvement in the pressure and the bearing load was obtained by increasing the lubricant's effective viscosity due to the dispersing of the nanoparticles. Using the CFD technique, Basim et al. [17] examined the impact of the bearing temperature, bearing deformation, and cavitation on the circular journal bearings' performance when lubricated with TiO_2 , Al_2O_3 , and CuO nano-lubricants. It was noted that the bearing pressure and the bearing load dropped while considering cavitation and elastic deformation. The temperature effect on a circular bearing lubricated with SAE15W40 distributed with various weight fractions of TiO_2 and ZnO nano-particles was studied by Yasir et al. [18] using the Kreger-Dougherty model to discuss the temperature and nanoparticles' impact on the lubricant viscosity. Aggregate ratios were evaluated experimentally using a dynamic light scattering test. A higher percentage of the nanoparticles added to the basic oil improved the bearing's load. It is obvious from a review of previous publications described above that little research has been done on the thermal behavior of elliptical bearings that have been lubricated with experimentally specified Nano-lubricants utilizing the CFD approach. The primary objective of the present work is to build a three-dimensional CFD model to investigate the static properties of the elliptical journal bearing when lubricated with experimentally characterized nano-lubricants, including a variable viscosity with temperature and nanoparticle concentrations. Since the lubricant viscosity affects the performance of the hydrodynamic bearings more than any other physical characteristics, a thorough evaluation is necessary. The viscosity of a Nano-lubricant depends primarily on the aggregate ratio, which varies depending on the type of lubricant in consideration. This ratio can be used to demonstrate how the type of nanoparticles utilized affects the performance of hydrodynamic bearings. The majority of the earlier studies used a constant value for this parameter. The two-step method synthesized the required TiO_2 and ZnO Nano-lubricants used in the present work. The aggregate ratio required for calculating the lubricant viscosity of such lubricants using the Kreger-Dougherty model was estimated experimentally using the dynamic light scattering test. Also, the density, thermal conductivity, and specific heat were taken as a function of nanoparticle concentration only.

2. NANO-LUBRICANT PREPARATION

The use of the Nano-lubricant is of great importance since it considerably enhances the performance characteristics of the investigated bearing. However, commercially available lubricants with aggregated nanoparticles have a significantly improved viscosity, which increases load-carrying capacity and can improve their tribological characteristics compared to other conventional

engine oils [19]. Hence, using the Nano-lubricant with the elliptical journal bearing was expected to improve its load-carrying capacity, which suffers compared to the circular journal bearing with a small expense in power dissipation. The Nano-lubricant used in the current investigation was made of 99% pure TiO_2 and ZnO nanoparticles sized 30 nm dispersed in SAE15W40 oil at varied concentrations. The following techniques were utilized to make such Nano-lubricants (it was extensively described in [18], and it will be repeated herein):

a. The nanoparticles were confirmed using the XRD test. Figures (1-a) and (1-b) show the results that were achieved.

b. SEM images of as-received ZnO and TiO_2 nanoparticles have been created and are shown in Figures 2-a and 2-b, respectively. ZnO nanoparticles are shaped like plates in Figure 2-a, whereas TiO_2 nanoparticles seem spherical in Figure 2-b. Although nanoparticle aggregates have average sizes of 58.54 nm and 51.05 nm, for ZnO and TiO_2 , respectively, they are still less than 100 nm in size.

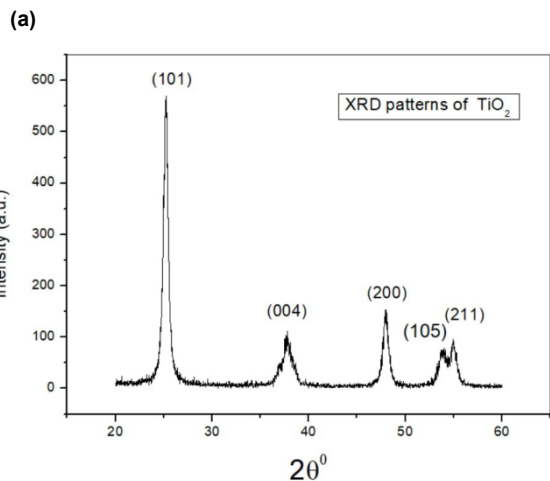
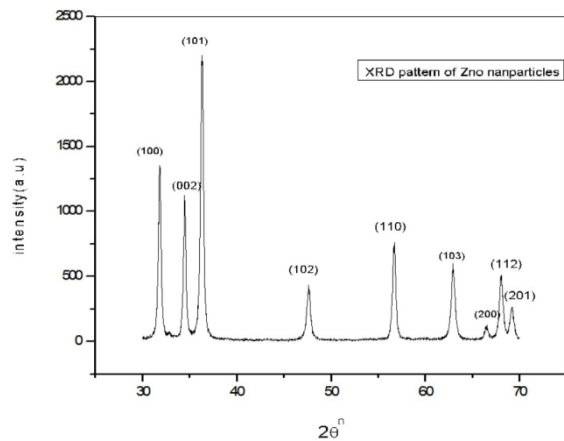
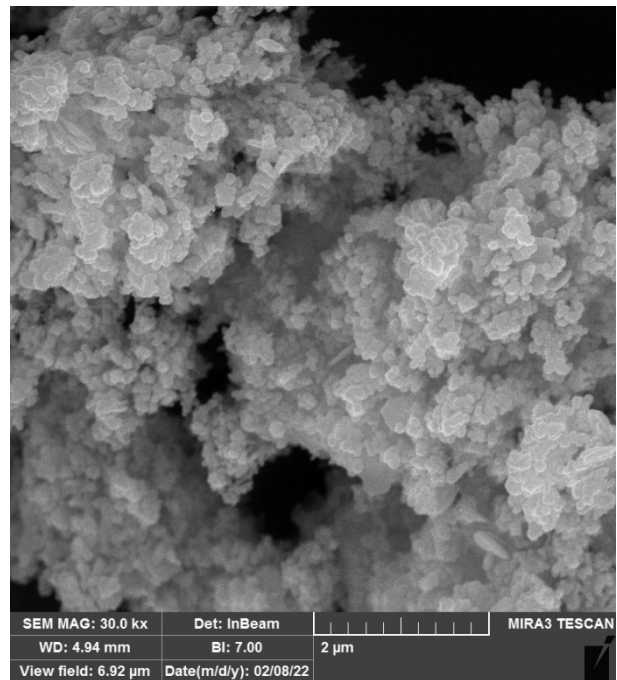


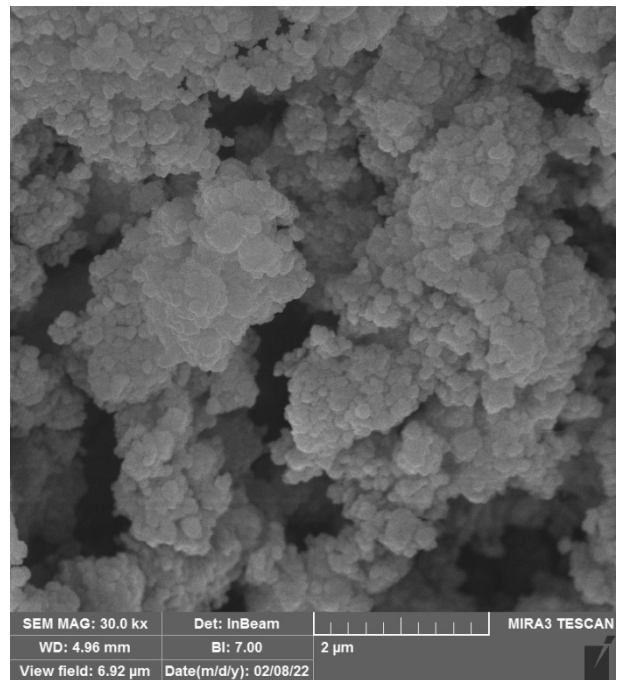
Figure 1. XRD of the nanoparticles (a) ZnO nanoparticles, (b) TiO_2 nanoparticles [18]

c. The SAE15W40 engine oil was dispersed with the 0.5, 1 and 2 wt% nanoparticles [18]. A surfactant (Olic acid) was used to achieve a uniform distribution of the nanomaterials and avoid precipitation.

d. The magnetic stirrer was used for mixing the produced Nano-lubricant for 1 h.



(a)



(b)

Figure 2. SEM image (a) ZnO nanoparticles (b) TiO_2 nanoparticles [18]

e. To prevent the anticipated agglomeration, a homogenizer type (MTI) was employed to sonicate the lubricant containing the dispersed nanoparticles at a frequency of (40 kHz) for 15 min at room temperature.

f. In order to assure good stability, the prepared Nano-lubricant was submitted right away for various necessary tests like dynamic light scattering (DLS) and viscosity studies.

g. The particle size distribution and aggregation ratios of the produced Nano-lubricants were calculated using dynamic light scattering (DLS). The outcomes are displayed in Figure 3.

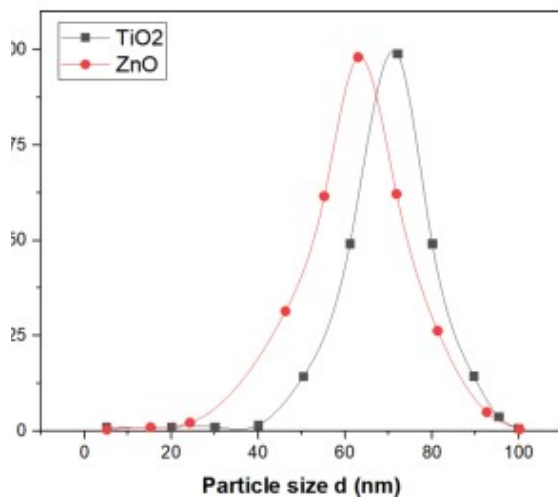


Figure 3. Particle size distribution of TiO₂ and ZnO Nanoparticles [18]

h. Figure 3 demonstrates that while the average aggregate size for TiO₂ nanomaterial is 72 nm, it is 62 nm for ZnO nanomaterial. The as-received nanoparticles' average size of (30 nm) is less than the diameters of the aggregated ZnO and TiO₂ nanoparticles. As a result, the aggregate ratios of the nanoparticles are 2.1 and 2.4, respectively.

3. CFD ANALYSIS

The next sections provide a detailed explanation of the mathematical model that was used to determine the pressure, temperature, and other bearing parameters.

3.1 Bearing Geometry

The elliptical journal bearing depicted in Figure 4 was examined in the present work. It consists of a stationary bush and journal with center O_j and radius R_j spinning at an appropriate speed with a small gap filled by the lubricant between them. The bearing circumferential coordinate is represented by θ . The eccentricity, lubricant viscosity, internal surface geometry, and gap between the journal and the bearing surfaces affect pressure growth inside elliptical journal bearings.

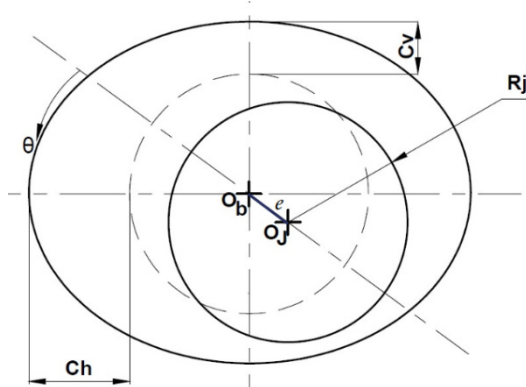


Figure 4. Schematic diagram of elliptical journal bearing

The EJB's oil film thickness can be expressed as follows [14]:

$$h = C_v \left(1 + \varepsilon \cos \theta + E_p \sin^2 (\theta + \phi) \right) \quad (1)$$

where:

$\varepsilon = \frac{e}{C_v}$ is the eccentricity ratio

E_p is the ellipticity ratio defined as:

$$E_p = \frac{C_h - C_v}{C_v}$$

3.2 Governing equations

The governing equations for Newtonian incompressible flow in an elliptical journal bearing with rigid walls operating in steady-state conditions are covered in this section. A thermo-hydro-dynamic study of such a bearing can be performed by solving the following continuity, momentum, and energy equations [20].

Continuity equation

$$\frac{\partial \rho}{\partial t} + \Delta(\rho \cdot \vec{v}) = 0 \quad (2)$$

where:

\vec{v} velocity lubricant vector

ρ lubricant density

For a steady state solution, the term $\partial/\partial t$ is turned off.

Momentum equations

The momentum equations are solved using FLUENT19. The equations are applied without body force and with variable properties with temperature and nanoparticle concentrations. They are unsteady and solved in the x, y, and z directions .

$$\frac{\partial}{\partial t}(\rho \cdot \vec{v}) + \nabla(\rho \cdot \vec{v} \cdot \vec{v}) = -\nabla P + \nabla(\bar{\tau}) + \rho \cdot \vec{g} + \vec{F} \quad (3)$$

where:

P is the static pressure

$\bar{\tau}$ is the stress tensor that can be evaluated as:

$$\bar{\tau} = \mu \left[\left(\nabla \cdot \vec{v} + \nabla \cdot \vec{v}^T \right) - \frac{2}{3} \nabla \times \vec{v} \cdot I \right] \quad (4)$$

where:

μ fluid viscosity

I Unit tensor

$\rho \cdot \vec{g}$ is the gravitational force

\vec{F} force due to gravity

The terms with $\partial/\partial t$ in this equation were turned off for steady-state analysis. The laminar flow assumption is assumed.

Energy equation

Solving the subsequent 3-D energy equation can calculate the oil film temperature[20].

Let:

$$A = \left(\frac{\partial T}{\partial t} + u \frac{\partial T}{\partial x} + v \frac{\partial T}{\partial y} + w \frac{\partial T}{\partial z} \right)$$

$$B = \left[\left(\frac{\partial u}{\partial y} \right)^2 + \left(\frac{\partial w}{\partial y} \right)^2 \right]$$

The energy equation can be written as:

$$\rho C_p A = \frac{\partial}{\partial y} \left(k \frac{\partial T}{\partial y} \right) + \mu B \quad (5)$$

Equation's (5) left side term stands for convectional heat transmission, whereas the right side term in this equation stands for viscous and conduction heat transfer. The terms with $\partial/\partial t$ in the equations were turned off for steady-state analysis.

3.3 Rheological and thermal characteristics of nano lubricants

The formulas listed below can be utilized for calculating the lubricants' rheological, physical, and thermal properties:

Viscosity of nano lubricants

The following modified Krieger-Dougherty model can be used to determine the lubricant's viscosity as a function of the nanoparticle volume fractions [21].

$$\mu_{nf} = \mu \left[1 - \frac{\varphi}{\varphi_m} \right]^{-[\eta]\varphi_m} \quad (6)$$

where:

φ_m : maximum fraction of particles packed. A value of 0.605 was chosen for φ_m as cited in [21]
 μ inherent (intrinsic) viscosity. It can be taken as 2.5, as cited in [21].

Substitution of φ_m and μ in equation (6) gives:

$$\mu_{nf} = \mu \left(1 - \frac{\varphi_a}{\varphi_m} \right)^{-2.5\varphi_m} \quad (7)$$

where;

$$\varphi_a = \varphi \left(\frac{a_a}{a} \right)^{3-D} \quad (8)$$

To compute the nano-lubricant viscosity, equation (9) can be used to convert the nanoparticle's mass fraction to the volume fraction [22].

$$\varphi = \left[\frac{\left(\frac{M_p}{\rho_p} \right)}{\left(\frac{M_p}{\rho_p} + \frac{M_f}{\rho_f} \right)} \right] \times 100 \quad (9)$$

where;

φ Volume percentage of the nanoparticles
 M_p Nanoparticles' mass
 M_f Pure oil's mass
 ρ_p , and ρ_f are the density of the nanoparticles and the pure oil

The following viscosity model can be used to analyze the temperature and nanoparticle concentration affecting the lubricant viscosity:

$$\mu = \mu_{nf} \exp[-\beta(T - T_i)] \quad (10)$$

Thermal conductivity of nano-lubricants

The following Maxwell model can be used to determine the nano lubricant's thermal conductivity as a function of its volume fractions [23]:

$$k_{nf} = k \left[\frac{(k_p + 2k) - 2\varphi(k - k_p)}{(k_p + 2k) + \varphi(k - k_p)} \right] \quad (11)$$

k is the thermal conductivity of the oil SAE15W40; it was taken as 0.13 W/m.K as cited in [24]

k_p is the nanoparticle's thermal conductivities.

Nano-lubricant density

The lubricant density as a function of the volume percentage of the nanoparticles can be evaluated as [23]

$$\rho_{nf} = (1 - \varphi)\rho_f + \varphi\rho_p \quad (12)$$

Specific heat

The effect of the nanoparticle's volume fraction on the lubricant-specific heat can be considered as [22]:

$$\rho_{nf} C_{p,nf} = (1 - \varphi)(\rho_f C_p) + \varphi(\rho C_p)_p \quad (13)$$

The TiO₂ and ZnO nanoparticle specifications are presented in Table 1.

Table 1. Nanoparticle properties [18]

Nanoparticles	TiO ₂	ZnO
Particle size	30 nm	30 nm
Purity	99.50%	99.80%
C _p (J/kg.K)	690	544
k(W/m.K)	8.3	19
ρ(kg/m ³)	4230	5606

4. BEARING PARAMETERS

The elliptical journal bearing's parameters can be evaluated as follows:

Load carrying capacity

The x and y- components of the bearing load can be deliberated as:

$$W_x = \int \int_{A_i} P_j \cdot \sin \theta \cdot (dA_j) \quad (14)$$

$$W_y = \int \int_{A_i} P_j \cdot \cos \theta \cdot (dA_j) = -W \quad (15)$$

the total bearing load can be determined as:

$$W = \sqrt{W_x^2 + W_y^2} \quad (16)$$

Friction force

The bearing friction force can be calculated as:

$$(F_{fr}) = \iint \tau \cdot (dA) \quad (17)$$

Power loss

The bearing power loss can be determined as follows:

$$H = fWU_j \quad (18)$$

Side leakage flow

The side leakage flow from both bearing sides can be presented as:

$$Q_s = \int_{\theta_1}^{\theta_2} \frac{h^3}{12\mu} \left(\frac{\partial P}{\partial z} \right)_{z=0,L} d\theta \quad (19)$$

5. BOUNDARY CONDITIONS AND COMPUTATIONAL PROCEDURE

The governing equations 2,3 and 5 are solved using the ANSYS FLUENT 19 program with the following assumptions and boundary conditions.

Boundary conditions

The following boundary for the fluid film can be assumed:

- The journal was reprinted as a moving wall with an absolute rotational speed.
- The bearing was modeled as a stationary wall.
- The two sides of the bearing are modeled as pressure outlets, as presented in Figure 5.
- The inlet pressure was set up as 101325 Pa.
- Coherent boundary condition at the bearing surfaces was adopted. This means that the velocity of the lubricant at the journal and the bearing are the same as the journal and bearing speeds.

Thermal boundary conditions required to solve the energy equation can be stated as follows:

- Through the interface between the fluid and solid zones, the temperature distribution in the fluid film is related to the solution of the temperature field in the solid bearing zone as follows:

$$-k_s \frac{\partial T_s}{\partial x_n} \Big|_{s;b} = h_{s;b} (T_{s;b} - T_f) \quad (20)$$

where s , b , and f refer to the shaft, bearing, and oil film, respectively. The temperature and heat transfer coefficient on the inner bearing and journal surfaces T_{sb} , T_b , h_s , h_b , are implicitly computed from the conjugate heat transfer rate between the fluid film field and the solid bearing zone.

- The side surfaces of the lubricant can be assumed at a constant temperature due to the thin layer of the lubricant as follows:

$$T = T_a z = \pm \frac{L}{2} \quad (21)$$

a refers to the ambient.

Computational procedure

The grid independence test illustrated in Figure 6 was conducted for a journal bearing $N=5000$ rpm and $\varepsilon=0.7$, lubricated with pure oil. The shape and the number of elements were chosen according to the results of the highest possible oil film pressure for such a bearing when tested with different elements. This figure demonstrated that a stable solution was attained when using 379200 hexahedral mesh elements with 0.5mm thickness and three layers in the radial direction. An element with an aspect ratio of 17.083 was used to ensure a good mesh quality.

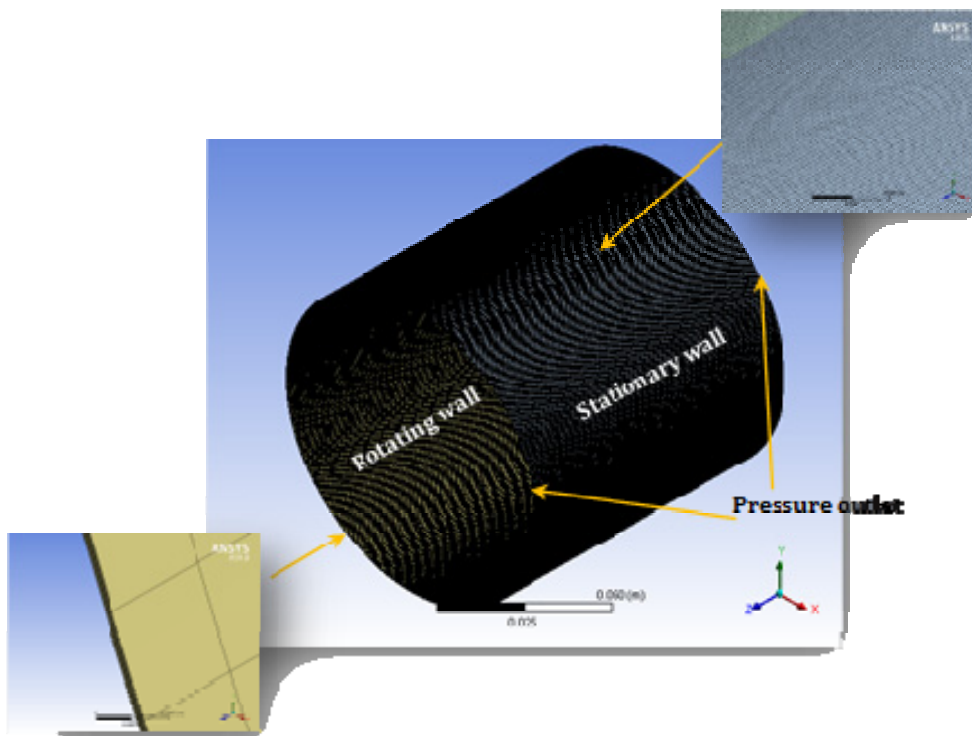


Figure 5. Grid and boundary of the fluid domain

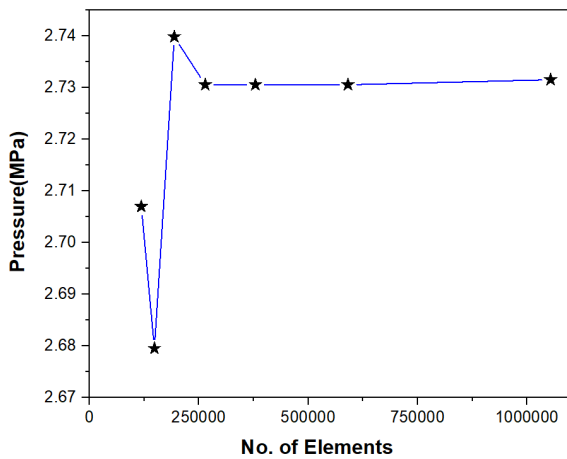


Figure 6. Grid Independences for a bearing working at N=5000 rpm and $\epsilon=0.7$

- The computational procedure can be illustrated below:
- Input parameters are specified in the design modeler using parametric sets.
 - The elliptical journal bearing with suitable dimensions is modeled using a CAD program.
 - The bearing model is imported to the ANSYS FLUENT-19 program. The fluid film of the bearing was discretized to finite-volume cells using the FLUENT program.
 - The viscosity variation with the temperature was included in the analysis using a suitable user-defined function (UDF) written in C⁺⁺.
 - The thermal conductivity, density, and specific heat as a function of nanoparticle volume fraction were also calculated.
 - The steady-state pressure solver is used with double precision.
 - During isothermal analysis, the energy equation is turned off while it is turned on during the thermal solution.
 - The velocity field and the preliminary user-preset pressure field were determined iteratively using the required boundary conditions.
 - A pressure correction equation is used to boost the pressure and velocity field, yielding interim resolutions to all conservation equations. The equations are iterated until they fulfill the convergence criterion. A convergence criterion of 10^{-4} was used for pressure and temperature.
 - The SIMPLC method is used in conjunction within a presto pressure environment for pressure velocity coupling. The "first-order upwind" with discernment scheme equation was used for each governing equation's convection terms, except that the PRESTO was used to solve the pressure (super-pressure option).
 - Pressure forces in X and Y directions were determined by utilizing "custom field functions".
 - All residual terms were given a convergence tolerance of 10^{-4} for better precision.

6. RESULTS AND DISCUSSION

The elliptical journal bearing the dimensions and operational parameters indicated in Table 2 has been modeled and studied numerically using the CFD

technique. The results obtained for the static performance of such a bearing under various working conditions, including the nanoparticle weight percentages, eccentricity ratios, ellipticity ratios, and journal speeds, are reported in this section.

Table 2. Bearing Dimensions and Operating Parameters

Parameter	Value	Parameter	Value
L/D	1	μ at 40°C	0.0985 Pa.s
R_i	50mm	β	0.0341/°C
C_v	0.1mm	ρ	877kg/m ³
Major Axis	100.4mm	C_p	2000J/kg.°C
Minor Axis	100.2mm	k	0.13W/m.°C
ϵ	0.3,0.5,0.7	wt.%	0.5,1,2
E_p	0.3,0.6,1	N	3- 5 krpm

Validation study

The validity of the EJB CFD model has been confirmed by contrasting some of the results obtained in the present work with those obtained by other researchers. The pressure distribution determined in this study for an EJB with an $\epsilon=0.7$ and N= 5000rpm lubricated with (AW32) pure oil was compared to that achieved by Dang et al. (2020). It demonstrated a good agreement, as illustrated in Figure 7-a.

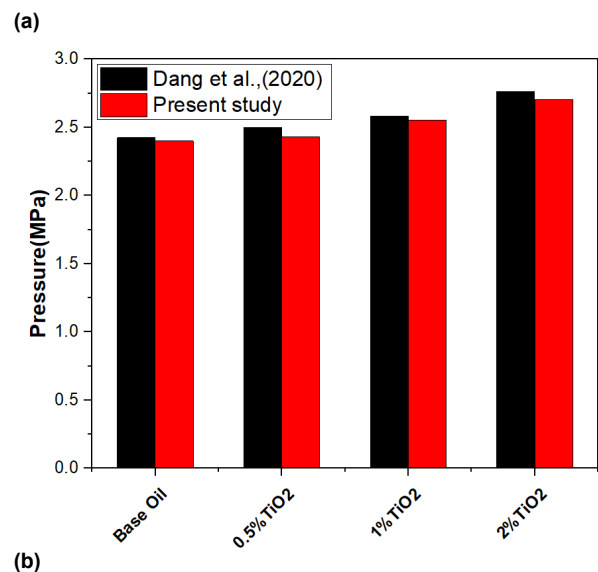
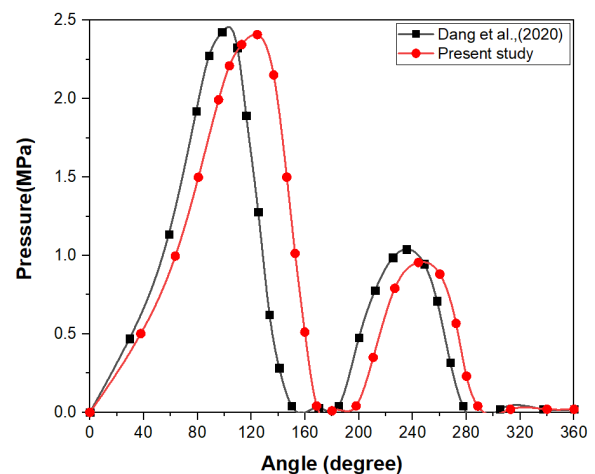
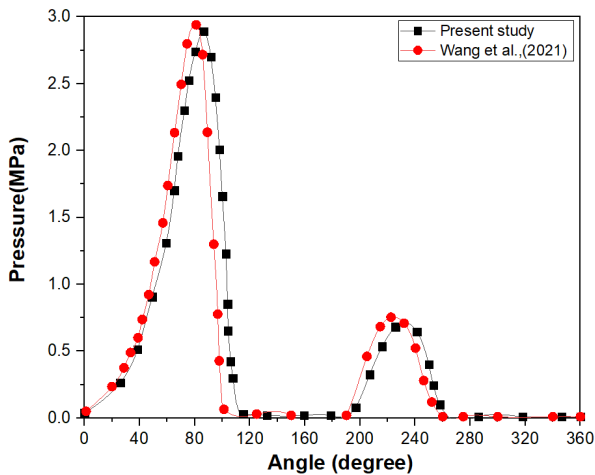
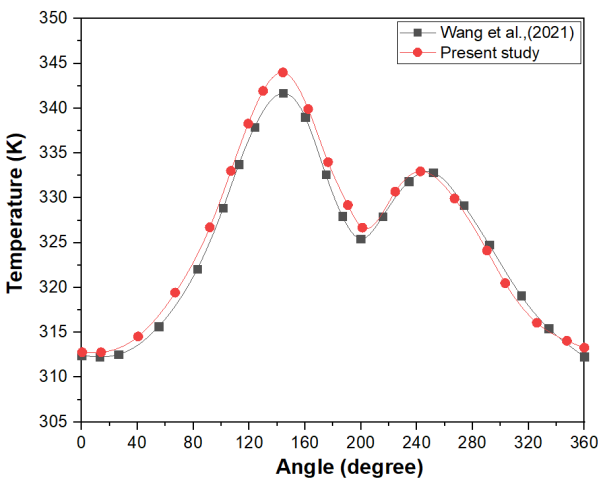


Figure 7. Verification of the EJB with Dang et al. (2021) (a) Oil film pressure (pure oil) (b) maximum oil film pressure(nano-lubricant)

Additionally, the maximum pressure obtained in the present work for an EJB with the same mentioned working conditions lubricated with 0.5wt%, 1wt%, and 2wt% TiO₂ nano-lubricant, was compared with that obtained by Dang et al. (2020), as illustrated in Figure 7-b. This figure illustrates obviously good agreement of the results, with a maximum deviation of 2.7%. The pressure and the temperature obtained in the present work for an EJB with a noncircularity ratio of 0.5, 0.1MPainlet pressure, and 3000 rpm shaft rotational speed lubricated with pure oil, were compared to the results obtained by Wang et al. (2021) as can be seen in figures 8-a and 8-b. These figures show a good agreement between the results, with maximum deviations for pressure and temperature of 1.38% and 1.47%, respectively.



(a)



(b)

Figure 8. Verification of the EJB results (a) pressure distribution (b) Oil film temperature

6.2 Effect of ellipticity ratio

The ellipticity ratio's impact on the key performance parameters of an EJB with $N=5000$ rpm and $\epsilon=0.7$ has been demonstrated in this section. The effect of the ellipticity ratio on the oil film thickness of the EJB lubricated with pure oil is illustrated in Figure 9. This figure shows that the oil film thickness becomes higher

for the bearing with a larger ellipticity ratio. Additionally, it can be observed from this figure that the oil film thickness at the upper lobe is greater than that of the lower lobe as a result of the higher horizontal clearance and the smaller vertical one. Figure 10 depicts how the ellipticity ratio affects the EJB oil film pressure distribution. This illustration shows that the elliptical bearing has two pressure lobes, with the pressure at the lower lobe being higher than that at the upper lobe.

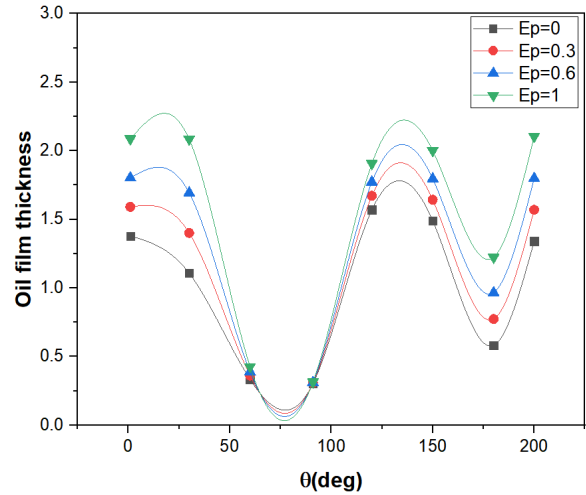


Figure 9. Effect of ellipticity ratio on the oil film thickness

Furthermore, the oil film pressure of the bearing exhibited the same behavior as the oil film thickness, with the pressure decreasing for the bearing with a larger ellipticity ratio due to the thicker oil film. This figure further demonstrates that, due to the reduction in the bearing's vertical clearance, the pressure at the lower lobe increases as the ellipticity ratio drops until it reaches 1.4 MPa for the bearing operating with an ellipticity ratio of 0.3. The bearing's oil film temperature additionally demonstrates the behavior of the oil film thickness, as can be seen in Figure 11. For a bearing with an increasing ellipticity ratio, the oil film thickness increases, causing a lower oil shear rate and friction force, leading to a drop in the oil film temperature. It is obvious that the bearing with the smaller ellipticity ratio achieved the highest oil film temperature.

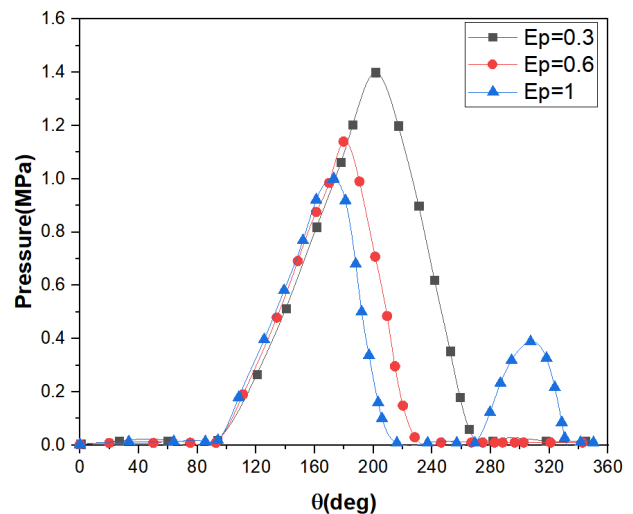


Figure 10. Effect of ellipticity ratio on the oil film pressure

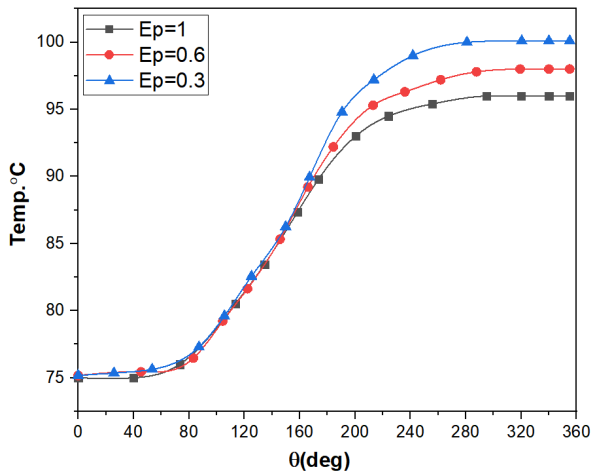


Figure 11. Effect of ellipticity ratio on the oil film temperature distribution, $\varepsilon = 0.7$, $N = 5000$ rpm

Figure 12 shows the TiO₂ and ZnO nanolubricated EJBload for various ellipticity ratios. This graph demonstrates that the bearing load falls for the bearing with a larger ellipticity ratio. This can be attributed to the increased oil film thickness and reduced oil film pressure. However, this figure shows that the bearing load increases with the addition of different weight fractions of nanoparticles in comparison to that lubricated with the oil without nanoparticles. It can also be observed that the oil dispersed with TiO₂ nanoparticles has a greater impact on the load than that dispersed with the ZnO nanoparticles. This can be explained by the fact that the TiO₂ nano-lubricant has a larger aggregate ratio than the ZnO nano-lubricant, which prevents the lubricant from flowing freely and causes a higher lubricant viscosity.

Figure 13 shows a decrease in the friction force of the EJB with increasing ellipticity ratios as a result of the lower shear rate associated with the higher film thickness. An increased viscosity of the nano-lubricants with the nanoparticle concentrations dispersed in the based oil causes a higher shear stress at the bearing surfaces and raises the friction force.

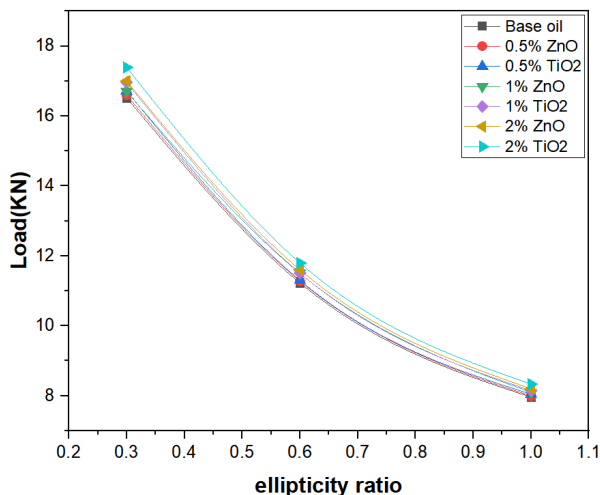


Fig.(12) Load carrying capacity vs. bearing ellipticity ratio and different particle concentration

Figure 14 demonstrates that the amount of oil that leaks out of the bearing's ends decreases for the bearing

with increasing ellipticity ratio as a result of lower oil film pressure at both ends. Further reduction in the side leakage flow was observed when using the nano-lubricants with a higher nanoparticle concentration as a result of the increased viscosity and greater resistance to the lubricant flow in this scenario.

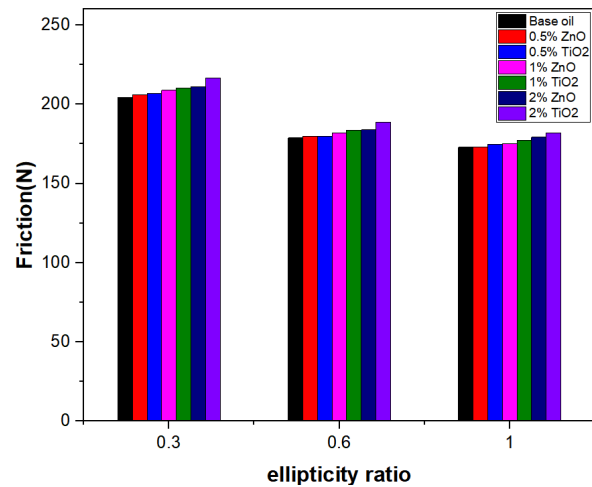


Figure 13. Effect of weight concentration and ellipticity ratio on the friction force

6.3 Journal speed effect

The effect of the journal speed on the maximum oil film pressure, temperature, and load-carrying capacity of the bearing was investigated while maintaining the ellipticity and eccentricity ratios at 0.6 and 0.7, respectively.

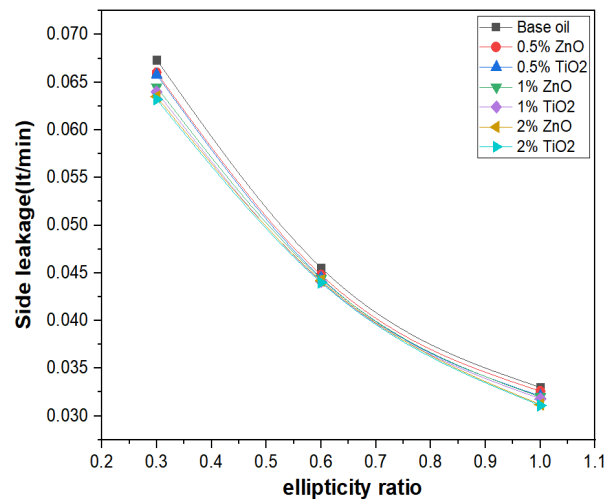


Figure 14. Effect of weight concentration and ellipticity ratio on the side leakage flow

The pressure contours for the EJB operating at various journal speeds (3000–5000 rpm) are shown in Figure 15 a–c. This figure shows that the bearing pressure rises with the rotational speed. The greatest bearing pressure increases from 1.04 MPa at a rotational speed of 3000 rpm to 1.1 and 1.15 MPa at a rotational speed of 4000 rpm and 5000 rpm, respectively.

Figure 16 illustrates how dispersing various nanoparticles in the base oil affected the greatest oil film pressure of the EJB. This figure also demonstrates how the journal speed marginally increased the maximum oil

film pressure within the bearing. Additionally, it has been shown that the dispersing of the nanoparticles into the base oil raised the maximum oil film pressure due to the higher viscosity of the nano-lubricant. The relatively small nanoparticle concentrations dispersed in the base oil were responsible for slightly improving maximum bearing oil film pressure.

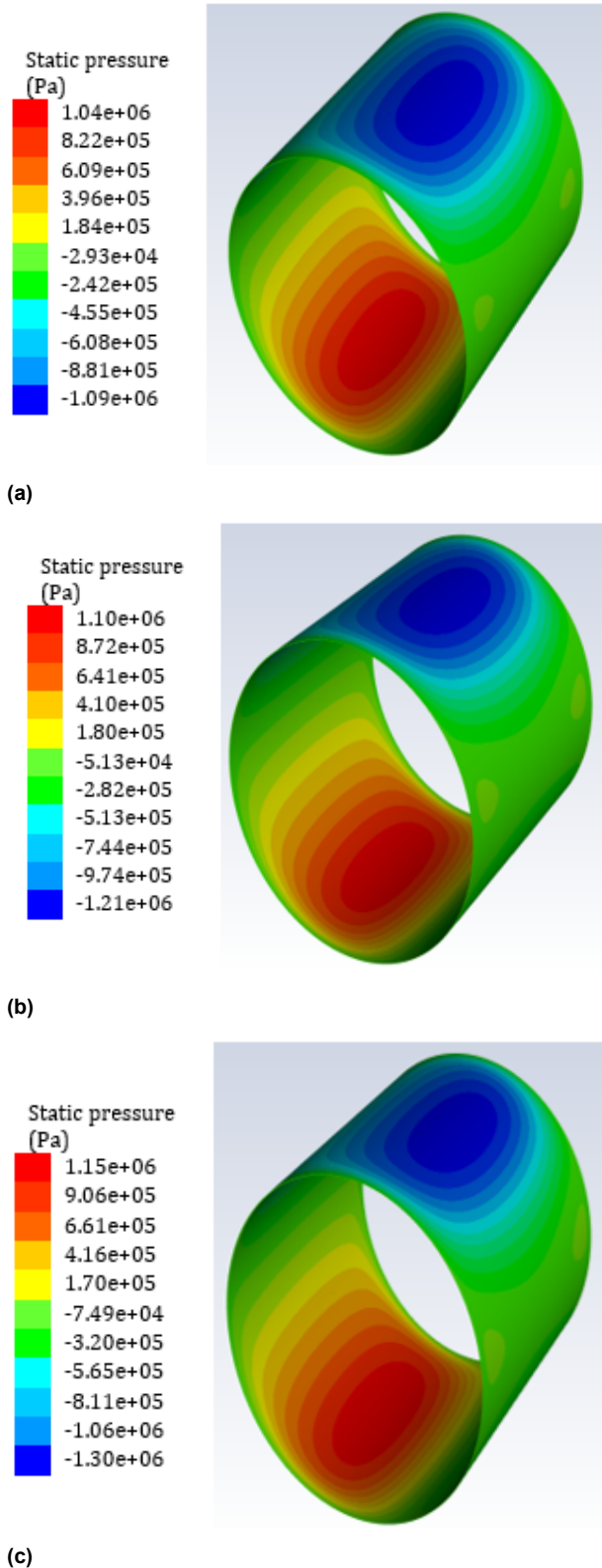


Figure 15. Pressure contours for a bearing with different journal speeds (a)N=3000rpm, (b) N=4000rpm, (c) N=5000rpm

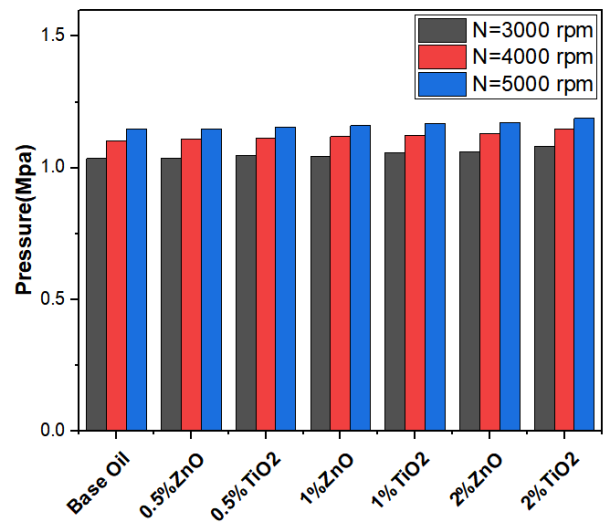


Figure 16. Effect of nanoparticle weight concentration and journal speed on the maximum pressure

Figure 17 demonstrated that the greatest bearing temperature grows by 22% and 26% when the journal speed increases to 4000 and 5000 rpm, respectively, in comparison with that operating at 3000 rpm. This is related to a higher lubricant shearing rate at faster journal speeds, resulting in higher shear stress and friction force, which is the main cause of bearing heat generation. Additionally, this figure shows that the nanoparticles dispersed in the base oil have a marginal effect on the maximum temperature.

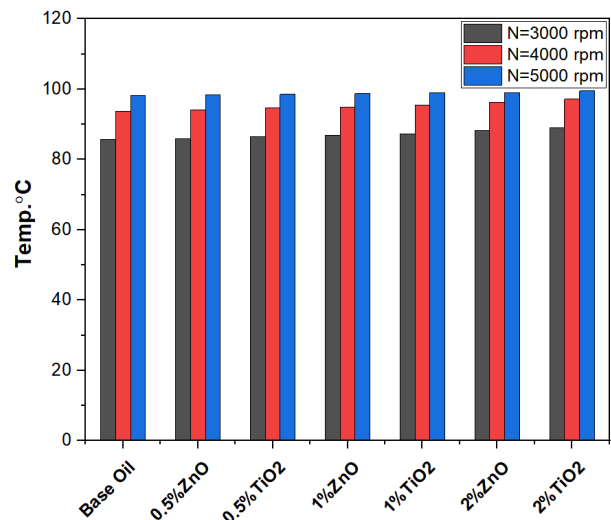


Fig17.Effect of weight concentration and journal speed on the maximum temperature

Figure 18 shows the combined effect of the journal speed and nanoparticle concentrations on the EJB's load-carrying capacity. The trend of this figure indicates that when the journal speed of the bearing is raised to 4000 or 5000 rpm compared to one operating at 3000 rpm, the load-carrying capacity increases by 10.6% and 20%, respectively. This is explained by how the bearing's wedge action increases in this situation. This figure obviously shows that the dispersing of the nanoparticles into the oil increased the viscosity of the nano-lubricant, which in turn increased the bearing's ability to carry more load. It should be noted that the addition of a small amount of nanoparticle to the pure

oil is what causes the minor increase in load-carrying capacity.

Eccentricity ratio effect

The eccentricity ratio effect on the performance of EJB was investigated by setting the bearing ellipticity ratio to 0.6 and the journal speed to 5000 rpm.

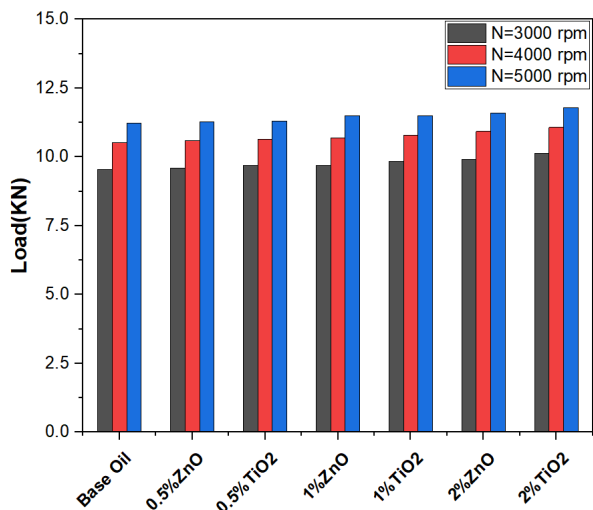


Figure 18. Effect of weight concentration and journal speed on the load-carrying capacity

The greatest pressure attained by the EJB operating at various eccentricity ratios and lubricated with pure oil and TiO₂ and ZnO nano-lubricants was illustrated in Figure 19. It was observed that the maximum oil film pressure becomes higher as the bearing works at higher eccentricity ratios. This can be explained by the small distance between the journal and the bearing surfaces (thinner oil film thickness) at the higher eccentricity ratio. Further growth in the bearing pressure was attained as a result of the higher viscosity of the nano lubricant. The maximum improvement in oil film pressure reaches 4% and 2.6% for the bearing lubricated with 2wt% of TiO₂ and ZnO nano lubricants, respectively, in contrast to that lubricated with the base oil. The increase of the TiO₂ nanolubricant viscosity can result from the larger aggregate ratio that inhibits the lubricant flow. The combined impact of the eccentricity ratio and nanoparticle concentration on the maximal temperature of the EJB is shown in Figure 20. This figure shows that the maximal temperature of the bearing was found to grow by 3.5% and 2.82%, respectively, due to using 2wt% of TiO₂ and ZnO nano-lubricants contrasted to that lubricated with the base oil. This can be attributed to the lower viscosity and higher thermal conductivity of the ZnO nano-lubricant compared to TiO₂ nano-lubricant.

Figure 21 depicts the load that the EJB was carrying while operating under the same circumstances mentioned earlier. This figure demonstrates that the thinner oil film thickness caused by, the higher eccentricity ratio raises the bearing load carrying capacity. This figure further demonstrated that the load increases when using nano-lubricants with higher nanoparticle concentrations. It has been demonstrated that the bearing load carrying capacity increased by 5.5% and 4% when

it was lubricated by 2 wt% TiO₂ and ZnO nanolubricants, respectively. When the EJB operates at greater eccentricity ratios, the friction force slightly increases as a result of the increased lubricant shear rate, as shown in Figure 22. The existence of TiO₂ and ZnO nanoparticles with different weight fractions causes further growth in the friction force due to the higher viscosity and, hence, the shear stress at the bearing surfaces. The maximum increase in friction force reaches 5.7% and 3.65% for 2 wt% of TiO₂ and ZnO nanolubricants, respectively.

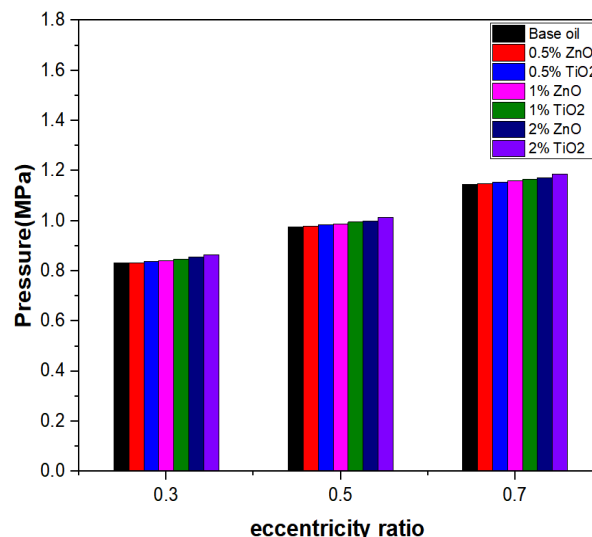


Figure 19. Oil film pressure vs. eccentricity ratio

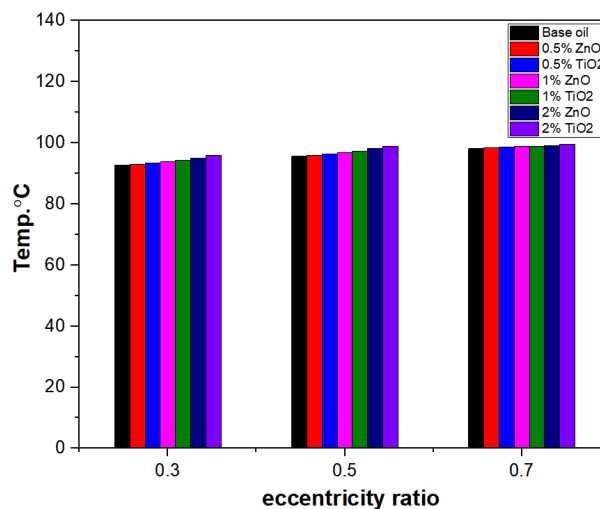


Figure 20. Temperature vs. eccentricity ratio

Figure 23 shows how the leakage flow from the bearing ends performed after it was lubricated with TiO₂ and ZnO nano-lubricants. The findings showed that the oil side leakage increases with the eccentricity ratios due to the higher oil film pressure at the bearing ends. However, the bearing leakage flow was reduced when the bearing was lubricated with nanolubricant. This can be attributed to the higher lubricant viscosity, which lowers its flow velocity. When the bearing was lubricated with 0.5% and 2 wt% TiO₂ nano-lubricants, the maximum decrease in side leakage was found to be 9% and 24.4%, correspondingly, while these percentages become 4.5% and 18.5% when using ZnO nano-lubricants with the same nanoparticle concentrations.

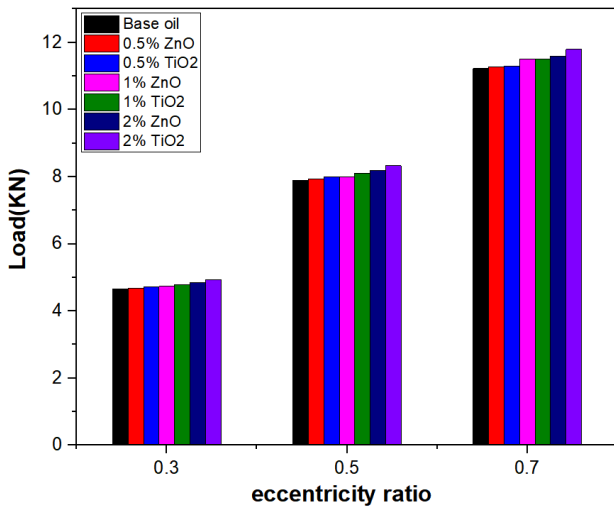


Figure 21. Effect of weight concentration and eccentricity ratio on the load-carrying capacity

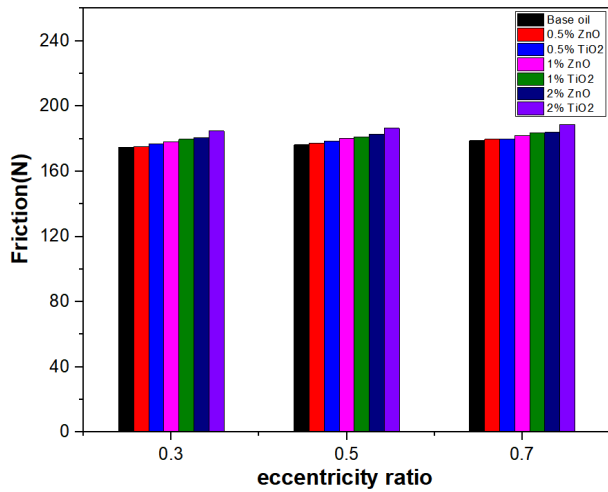


Figure 22. Effect of weight concentration and eccentricity ratio on the friction force

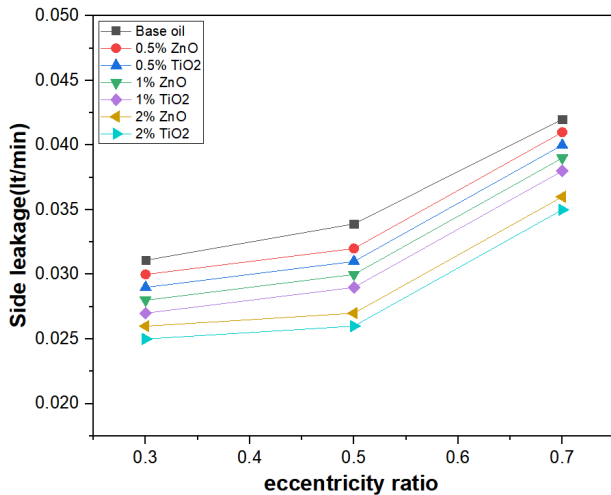


Figure 23. Effect of weight concentration and eccentricity ratio on the side leakage flow

Figure 24 depicts the combined effects of the eccentricity ratio and ZnO and TiO₂ nanoparticle concentrations on the EJB's power loss. This figure demonstrates how the power loss slightly rises with the eccentricity ratio of the bearing. Additionally, the power loss is increased due to the nanoparticle dispersion.

It was noted that the power loss increased by 5.7% and 4.18% when using 2wt% of TiO₂ and ZnO nano lubricants, respectively.

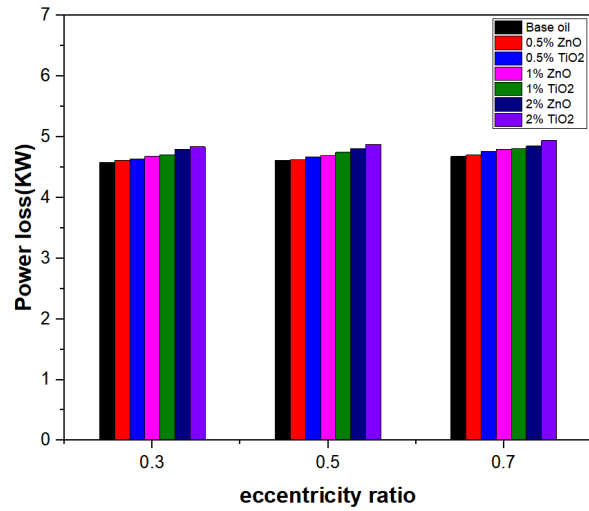


Figure 24. Effect of weight concentration and eccentricity ratio on the power loss

7. CONCLUSIONS

As the bearing was developed, lubrication has been widely acknowledged as being essential to maximizing performance. Nanoparticles, which are extremely tiny particles, have the ability to produce tribo-films, penetrate small asperities of moving surfaces, and enhance tribological properties. Nanoparticles' rolling motion decreases wear and friction losses, which further boosts the system's effectiveness. So, the current study represents an attempt to study the effects of using nano-lubricants on the performance of one of the most important noncircular bearings (Elliptical journal bearing). The properties of an EJB lubricated with experimentally established TiO₂ and ZnO nano-lubricants were investigated using a 3D-CFD model with the ANSYS-FLUENT19 program. With the available published data, the CFD model employed in the current work was successfully and confidently confirmed. The investigation indicated that adding nanoparticles to base oil improved both the bearing maximal pressure and the load that supported it. The increase becomes higher with the higher nanoparticle concentrations added to the base oil. The TiO₂ nanolubricant reveals higher pressure and load capacity values than the ZnO nano-lubricant. In general, the dispersion of the nanoparticles into the base oil has little effect on the oil film temperature compared to the bearing load. Power loss rises with the dispersion of the nanoparticles in the oil. The higher the nanoparticle concentration, the higher the power loss.

Moreover, the side leakage of the lubricant always decreases with the addition of the nanoparticles. It becomes lower when using a lubricant with a higher nanoparticle concentration. The bearing pressure, temperature, and load-carrying capacity always increased with the journal speed. The oil film pressure, temperature, load-carrying capacity, side leakage, and friction all decreased as the ellipticity ratio of the

bearing increased while the eccentricity ratio remained constant.

In general, the present work provides an efficient CFD method to examine the performance of an elliptical journal bearing that has been lubricated with TiO₂ and ZnO nano-lubricants using ANSYS-FLUENT software. The current study recommends this approach to reduce experimental effort and assist bearing designers.

The present work can be extended to investigate the effect of using PTFE and MoS₂ nanoparticles and their hybrid on the static performance of such a bearing.

REFERENCES

- [1] Hussain, A., Mistry, K., Biswas, S., and Athre, K.: Thermal Analysis of Noncircular Bearings. *Journal of Tribology*, Vol.118, No.1, pp. 246–254,1996. <https://doi.org/10.1115/1.2837086>
- [2] Mishra, P. C.: Thermal analysis of elliptic bore journal bearing. *Tribology Transactions*, Vol.50, No.1, pp.137–143, 2007. <https://doi.org/10.1080/10402000601105573>
- [3] Chauhan, A., Sehgal, R., &Sharma, R. K.: Thermohydrodynamic analysis of elliptical journal bearing with different grade oils. *Tribology International*, Vol.43, No.11, pp.1970–1977, 2010. <https://doi.org/10.1016/j.triboint.2010.03.017>
- [4] Sehgal, R.: Experimental Measurement of Oil Film Temperatures of Elliptical Journal Bearing Profile Using Different Grade Oils. *Tribology Online*, Vol.5, No.6, pp.291–299, 2010. <https://doi.org/10.2474/trol.5.291>
- [5] Sehgal, R., Chauhan, A., Sharma, R. K.: An experimental investigation of oil film temperatures in elliptical profile journal bearing. *Tribology Online*, Vol.8, No.1, pp.1–6, 2013. <https://doi.org/10.2474/trol.8.1>
- [6] Susilowati, S., Hilmy, F., Arfiandani, D., Muchammad, Tauviqirrahman, M., & Jamari, J.: Effect of eccentricity ratio on the hydrodynamic performance of journal bearing considering cavitation. *AIP Conference Proceedings*, 2097, April 2019. <https://doi.org/10.1063/1.5098243>
- [7] Singla, A., Chauhan, A.: Evaluation of oil film pressure and temperature of an elliptical journal bearing - An experimental study. *Tribology in Industry*, Vol.38, No.1, pp.74–82, 2016.
- [8] Susilowati, Tauviqirrahman, M., Jamari, J., Bayuseno, A. P., and Muchammad.: A comparative study of finite journal bearing in laminar and turbulent regimes using CFD (computational fluid dynamic). *MATEC Web of Conferences*, 58, 2016. <https://doi.org/10.1051/mateconf/20165804001>
- [9] Ebrahimi, A., Akbarzadeh, S., and Moosavi, H.: Geometrical analysis of elliptical journal bearings and its effects on friction and load capacity. *Proceedings of the Institution of Mechanical Engineers, Part J: Journal of Engineering Tribology*, Vol. 234, No.5, pp. 743–750, 2020. <https://doi.org/10.1177/1350650119868090>
- [10] Kumar, M., Chandravanshi, M. L., & Mishra, P. C.: Geometrical analysis of elliptical journal bearing lubricated with Newtonian fluid. *AIP Conference Proceedings*, 2341, May 2021. <https://doi.org/10.1063/5.0050234>
- [11] Bhaskera, B., Seetharamaiahb, N., & Babu, P. R.: Experimental investigations on elliptical journal bearing using hydrol 68 lubricating oil. *AIP Conference Proceedings*, 2317, February 2021. <https://doi.org/10.1063/5.0036458>
- [12] Wang, L., Geng, H., Zhang, W., Ge, X., & He, M.: Effect of Ellipticity on Cavitation Mechanism and Thermal Effect of Elliptical Journal Bearings. *Tribology Online*, Vol.16, No.4, pp.279–285, 2021. <https://doi.org/10.2474/trol.16.279>
- [13] Kedzierski, M. A.: Viscosity and density of aluminum oxide nanolubricant. *International Journal of Refrigeration*, Vol. 36, No.4, pp.1333–1340, 2013. <https://doi.org/10.1016/j.ijrefrig.2013.02.017>
- [14] Dang, R. K., Chauhan, A., and Dhami, S. S.: Static thermal performance evaluation of elliptical journal bearings with nanolubricants. *Proceedings Journal of Engineering Tribology*, Vol. 235, No.8, pp. 1627–1640, 2020. <https://doi.org/10.1177/1350650120970742>
- [15] Saba.Y. Ahmed, Basim A. Abass, Zainab H. Kadhim.: CFD analysis of thermo-hydrodynamic behavior of nano-lubricated journal bearings considering cavitation effect, *Journal of the Serbian Society for Computational Mechanics*, Vol.15, No. 1, pp.110-130,2021. <https://doi.org/10.24874/jssc.m.2021.15.01.08>
- [16] Abolfazl Rasoolizadeh Shooroki, Asghar Dashti Rahmatahadi, Mahdi Zare Mehrjardi.: Effect of using hybrid nano lubricant on the thermo-hydrodynamic performance of two lobe journal bearings, *Proceedings of the Institution of Mechanical Engineers, Part J: Journal of Engineering Tribology*, Vol. 236, No.6, 2022. <https://doi.org/10.1177/13506501211053089>
- [17] Basim A. Abass · Saba Y. Ahmed · Zainab H. Kadhim.: Thermoelasto-Hydrodynamic Analysis of Nano-lubricated Journal Bearings Using Computational Fluid Dynamics with Two-way Fluid-Structure Interaction Considering Cavitation, *Arabian Journal for Science and Engineering*, published on line 20 July, 2022 <https://doi.org/10.1007/s13369-022-07024-9>
- [18] Yasir, M. O., Ahmed, S. Y., Abass, B. A.: Performance Analysis of Experimentally Characterized Titanium Dioxide and Zinc Oxide Nano-Lubricated Journal Bearing Considering Thermal and Cavitation Effects. In *Arabian Journal for Science and Engineering*, Sept.2022. <https://doi.org/10.1007/s13369-022-07219-0>
- [19] S.K. Mandal, B. Bhattacharjee, K. Choudhuri, P. Chakraborti.: Application of nanofluids on various performance characteristics of hydrodynamic journal bearing-A review, *Proceedings of the Institution of Mechanical Engineers, Part E: Journal of Pro-*

cess Mechanical Engineering, 2021. <https://doi.org/10.1177/09544089211063995>

- [20] H.K. Versteeg, W. Malalasekera.: An Introduction to Computational Fluid Dynamics. In IEEE Concurrency, vol. 6, No. 4, 2007. <https://doi.org/10.1109/mcc.1998.736434>
- [21] Krieger, I. M., Dougherty, T. J.: A Mechanism for Non-Newtonian Flow in Suspensions of Rigid Spheres. Transactions of the Society of Rheology, Vol.3, No.1, pp.137–152,1959. <https://doi.org/10.1122/1.548848>
- [22] Azmi, W. H., Sharma, K. V., Sarma, P. K., Mamat, R., Anuar, S., & Dharma Rao, V.: Experimental determination of turbulent forced convection heat transfer and friction factor with SiO₂ nanofluid. Experimental Thermal and Fluid Science, Vol. 51, pp.103–111, 2013. <https://doi.org/10.1016/j.exptthermflusci.2013.07.006>
- [23] Maneshian, B., & Nassab, S. A. G.: Thermo-hydrodynamic analysis of turbulent flow in journal bearings running under different steady conditions. Proceedings of the Institution of Mechanical Engineers, Part J: Journal of Engineering Tribology, Vol.223, No.8, pp.1115–1127, 2009. <https://doi.org/10.1243/13506501JET575>
- [24] T.N. Jaber, K.A. Sukkar, A.A Karamalluh: Specifications of Heavy Diesel Lubricating Oil Improved by MWCNTs and CuO as Nano-additives, 1st International Conference on Petroleum Technology and Petrochemicals, IOP Conf. Series: Materials Science and Engineering 579 (2019) 012014, <https://doi.org/10.1088/1757899X/579/1/012-014>

NOMENCLATURE

C_v	Vertical clearance of the elliptical bearing
C_h	Horizontal clearance of the elliptical bearing
C_p	Specific heat of the lubricant
$(C_p)_p$	Specific heat of the nanoparticles
$(C_p)_{nf}$	Specific heat of the nano lubricant
f	The coefficient of friction
H	The power loss (Watt)
k	Thermal conductivity of the lubricant
k_p	Thermal conductivity of the nanoparticles
k_{nf}	Thermal conductivity of the nano lubricant
T	Temperature of the oil film
T_i	The inlet oil film temperature
U_j	The journal surface speed(m/sec)
W	The applied load (N)

Greek symbols	
β	Lubricant viscosity-temperature coefficient C ⁻¹
Φ	Attitude angle(degree)
M	Base oil viscosity(N.s/m ²)
μ_{nf}	The viscosity of the nano-lubricant (N.s/m ²)
Φ	The volume fraction of nanoparticles
ρ_f	The density of the pure oil(kg/m ³)
ρ_p	The density of the nanoparticles(kg/m ³)
ρ_{nf}	The Nano lubricant density(kg/m ³)
Superscripts	
f	Fluid (lubricant)
p	Nanoparticle
nf	Nanofluid (Nanolubricant)

Abbreviations

XRD	X-Ray Diffraction
SEM	Scanning electron Microscope

АНАЛИЗА ПЕРФОРМАНСИ ЕЛИПТИЧНОГ ЛЕЖАЈА ПОДМАЗАНОГ ЕКСПЕРИМЕНТАЛНО КАРАКТЕРИЗОВАНИМ НАНО-МАЗИВОМ С ОБЗИРОМ НА ТОПЛОТНИ ЕФЕКАТ КОРИШЋЕЊЕМ ЦФД ТЕХНИКЕ

Б.А. Абас, С.Ј. Ахмед, М.А. Јасер

Ова студија користи рачунарску динамику флуида (ЦФД) за квантитативно испитивање перформанси елиптичног клинастог лежаја (ЕЈБ) подмазаног нано-мазивом TiO₂ и ZnO с обзиром на термички ефекат. У експерименту, наночестице са концентрацијом честица које варирају од 0 до 2 тежинских процента се мешају са моторним уљем SAE15B40 да би се створила ова мазива. Испитан је утицај тежинских удела, брзине ротације, ексцентрицитета и елиптичности на термичке перформансе ЕЈБ-а. Крегер-Доугхерти модел се користи за разумевање ефеката температуре уљног филма као и концентрације наночестица на вискозитет мазива. Притисак и температура утврђени помоћу (Данг 2020) и (Ванг 2021) су процењени у односу на ЦФД модел са добрим слагањем. Налази показују да је за 2 wt% наночестица, ϵ од 0,6 и H од 5000 о/мин, носивост повећана за 5,5 % и 4%, а бочни проток цурења је смањен за 24,4% и 18%.